JOURNAL OF NANOSTRUCTURED POLYMERS AND NANOCOMPOSITES **8**/4 119-126

SILSESQUIOXANES FUNCTIONALIZED WITH ONE OR TWO SIDE-CHAIN AMINO GROUPS AS COINITIATORS OF CAMPHORQUINONE IN PHOTO-INITIATED POLYMERIZATION OF METHACRYLATE MONOMERS

Ignacio E. dell´Erba, Silvana V. Asmussen, Walter F. Schroeder, Claudia I. Vallo*

Institute of Materials Science and Technology (INTEMA), University of Mar del Plata, CONICET
Juan B Justo 4302, 7600 Mar del Plata, Argentina.

Received 7 May 2012; Accepted 16 October 2012

Abstract
Organotrialkoxysilanes (APS-PGE2) and (DAS-PGE3) were synthesized by reacting 1 mole of 3-(aminopropyl)triethoxysilane (APS) with 2 mole of phenylglycidylether (PGE) or 1 mole of N-(β-aminoethyl)-γ-aminopropyltrimethoxysilane (DAS) with 3 mole of PGE respectively. Polyhedral oligomeric silsesquioxanes functionalized with bulky amino groups (ASSQO) were prepared by hydrolytic condensation of both APS-PGE2 and DAS-PGE3 using formic acid a a catalyst. The polymerization of methacrylate resins photoinitiated by camphorquinone (CQ) in combination with the synthesized ASSQO was investigated. The progress of monomer conversion vs. irradiation time showed that the CQ/ASSQO pair constitutes an efficient photoinitiator system because a fast reaction and high conversion result from 60 s irradiation at 600 mW/cm^2. The mechanical behaviour of these systems in flexural and compressive tests was highly dependent on the structure of the ASSQO.

Keywords: Silsesquioxanes; Nanocomposites; Photoinitiator; Mechanical properties.

1. Introduction

Light-activated dental composites are widely used in clinical restorative dentistry. In these materials, photopolymerization is commonly activated by visible light, using an initiator system comprising a α-diketone in combination with an amine reducing agent. It has been proposed that in these bimolecular systems, the interaction of the photoinitiator with the amine involves an electron-transfer process, from which reactive radicals are produced [1]. The camphorquinone (CQ)/amine photo-initiating system is the most common one used in the current photoactivated dental materials, which produces free radicals on exposure to 450-500 nm radiation [2-5]. The efficiency of this system affects clinically important properties such as polymerization rate, depth of cure and final monomer conversion.

The tertiary amine derivatives used as coinitiator in light-cured dental restorative resins are both toxic and mutagenic. However, they are a necessary component of the visible-light photoinitiator system based on camphorquinone. The toxicity of restorative materials containing amines as a co-initiator is connected with the mobility of the amine molecule if other components are essentially non-toxic. Some polymeric or macromolecular photoinitiators (or coinitiators) have been reported to have significant advantages over commercially available low molecular weight photoinitiators, such as good solubility and compatibility in the curable medium, low toxicity due to the well-known polymer effect [6–8]. The use of high molecular weight photoinitiators reduces the tendency to migrate owing to their macromolecular nature. Additional ways of reducing its leaching into tissue are the use of polymerizable amines that are incorporated into the polymer chain [8] or the increase of the molecular size by using bulky substituent so that it does not diffuse out of the resin.

To reduce the toxicity and improve the polymerization process, the nanocomposite materials based on polyhedral oligomeric silsesquioxanes (SSQO) are an interesting alternative because of the unique features derived from the introduction of appropriated functionalities (for instance amines) in the organic branches of the SSQO, in addition to its biocompatibility associated to the large molecular size. Polyhedral oligosilsesquioxanes are an interesting class of clusters derived from the hydrolytic condensation of trifunctional organosilicon monomers. As illustrated in Scheme 1, SSQO molecules are cage-like organic–inorganic structures, which consist of a Si–O–Si inorganic cage surrounded by organic branches. The inorganic cage may be a fully condensed closed structure of formula $(RSiO_{1.5})_n$, (R represents the organic substituents) or partially con-

Corresponding author E-mail: civallo@fi.mdp.edu.ar

densed open structure of generic formula $T_n(OH)_m$, where $T=RSiO_{1.5-m/2n}$. The diameter of these structures ranges from 1 to 3 nm, depending on the number of silicon atoms in the central cage and the peripheral substitution groups surrounding this core. The SSQO unit can be viewed as a nanoparticle for both its size and filler function, or as a co-initiator for its ability to initiate photopolymerization. The interest in SSQO has rapidly grown over the past several years, particularly for polymer-related applications, where several families of SSQO monomers have been developed as precursors to hybrid inorganic–organic polymers [9-11]. The affinity of polyhedral oligosilsesquioxanes to various polymer materials can be easily controlled by the selection of the structure of the surrounding organic group [12]. Methacrylate [13-14], epoxy [15-16], amine [17], and (β-carboxyl) ester [18] are some examples of functional groups that have been incorporated into the organic part of silsesquioxanes in order to optimize the molecular structure of cubic-oligosilsesquioxane according to different objectives.

To our knowledge, the use of tertiary amine-functionalized silsesquioxanes (ASSQO) as components of visible-light photoinitiator systems has not been previously reported in the scientific literature. The present study describes the synthesis of two different ASSQO and analyzes the performance of them as coinitiators of CQ in visible-light photopolymerization. The influence of the structure of the ASSQO on the final mechanical properties of materials prepared from a dimethacrylate monomer is analyzed. Characterization of the polymerized materials was carried out by measuring flexural and compressive properties.

2. Experimental

2.1. Materials

The resins were formulated from blends of 2,2-bis[4-(2-hydroxy-3-methacryloxypropoxy)phenyl]propane (bis-GMA; Esstech, Essington, PA) and triethylene glycol dimethacrylate (TEGDMA; Aldrich) at mass percentage of 70 : 30. The 70 : 30 bis-GMA/TEGDMA blend is denoted BisTEG. 3-(aminopropyl)triethoxysilane (APS, Sigma, 98% purity), N-(β-aminoethyl)-γ-aminopropyl trimethoxysilane (DAS, Sigma, 98% purity), Phenylglycidylether (PGE, Aldrich, 99% purity), formic acid (85 wt.% Sigma), Camphorquinone (Aldrich, 98% purity) and ethyl-4-dimethylaminobenzoate (EDMAB, Aldrich, 98% purity) were employed as received. The resins were activated for visible light polymerization by the addition of 1 wt% CQ in combination with the synthesized amine-functionalized silsesquioxanes.

The radiation source was a light-emitting diode (LED) unit (VALO, Ultradent, USA) with a wavelength range from 410 nm to 530 nm and an irradiance equal to 600 mW/cm^2. The intensity of the LED was measured with the chemical actinometer potassium ferroxialate, which is recommended for the 253–577 nm wavelength range.

2.2. Characterization

2.2.1. Photolysis of CQ in the presence of ASSQO

The photodecomposition of CQ in the presence of ASSQO was followed by using the changes in absorbance at the wavelength of its maximum absorption. The absorption spectra of CQ were measured with a UV-visible spectrophotometer (1601 PC, Shimadzu) at room temperature (ca 20 °C) in BisTEG resin. Photobleaching experiments were carried out in 2.0 ± 0.2 mm thick samples sandwiched between two disposable 1 mm thick glass plates. The concentration of CQ in BisTEG resin was 1 wt% and the ASSQO were used in different mass fractions. The APS-derived silsesquioxanes (ASSQO1) were incorporated in proportions 7.5, 15 and 30 wt%, and the DAS-derived silsesquioxanes (ASSQO2) in proportions equal to 5.5, 11 and 22 wt% to BisTEG resin. The extinction coefficient of CQ in methacrylate resin was 42 L mol^{-1} cm^{-1}.

2.2.2. Measurement of double bond conversion

Fourier transform infrared (FTIR) spectra were acquired with a Nicolet 6700 Thermo Scientific. Near-infrared (NIR) spectra were acquired over the range 4500-7000 cm^{-1} from 16 co-added scans at 2 cm^{-1} resolution. The resins were sandwiched between two glass plates separated by a 2 mm rectangular rubber spacer and were tightly attached to the sample holder using small clamps. With the assembly in a vertical position, the radiation source was placed in contact with the glass surface. The specimens were irradiated at regular time intervals and spectra were collected immediately after each exposure interval. The background spectra were collected through an empty mould assembly fitted with only one glass slide to avoid internal reflectance patterns. The conversion profiles were calculated from the decay of the absorption band located at 6165 cm^{-1}.

2.2.3. Mechanical characterization

Flexural and compressive tests were carried out at room temperature (20 ± 2 °C) in an Instron testing machine (Model 4467) at a crosshead displacement rate of 2 mm/min. Prior to mechanical testing, the specimens were stored for about 24 h. A set of test

specimens was also post-cured at 120 °C for 2 h. The flexural modulus, E, and the flexural strength, σ_f were measured in three-point bending using sample dimensions recommended by the ISO 4049:2000(E): (25±2) mm ×(2±0.1) mm ×(2±0.1) mm. A minimum of four specimens were prepared for each system by photo curing the specimens at 600 mW/cm^2 for 1 min on each side.

Multifunctional methacrylates are brittle in nature. Like other brittle materials, they are weak in tension but quite strong in compression and capable of yielding under uniaxial compression. Therefore, the yield strength was determined in compression. Samples for compression testing were made by injecting the resins into polypropylene cylindrical disposable moulds of 6 mm internal diameter. Samples were irradiated at 600 mW/cm^2 for 1 min on each side. The shrinkage during polymerization facilitated the removal of the specimens from the polypropylene mould. Prior to mechanical testing, the specimens were stored at room temperature for about 24 h. Cylindrical specimens having a length/diameter ratio of 1.5 were deformed between metallic plates lubricated with molybdenum disulfide. The deformation was calculated directly from the cross-head speed. True stress–deformation curves were obtained by dividing the load by the cross-sectional area. The compressive yield strength, σ_y, was determined at the maximum load.

3. Results and discussion

3.1 Synthesis of amine-functionalized silsesquioxanes (ASSQO).

Organotriethoxysilanes containing one amino group were synthesized by reacting 1 mole of APS with 2 mole of PGE to give APS-PGE2 [19, 20]. Organotrimethoxisilanes functionalized with two bulky amino groups were prepared from 1 mole of starting aminosilane DAS by reaction with 3 mole of PGE to give DAS-PGE3 [21, 22]. The reactions were carried out in glass tubes sealed under vacuum and placed in a thermostat held at 50 °C, during 24 h.

The hydrolytic condensation of organotrialkoxysilanes, $RSi(OR')_3$ where R and OR´ represent an organic and an alkoxy group respectively, leads to products that are generically called poly(silsesquioxanes) or silsesquioxanes (SSQO) [22]. Species present in a SSQO may vary from perfect polyhedra of formula $(RSiO_{1.5})_n$ (n is an even number ≥ 6), to partially condensed (but completely hydrolyzed) products of generic formula $T_n(OH)_m$, where $T=RSiO_{1.5-m/2n}$. The hydrolytic condensation of the organotrialkoxysilanes containing one amino group (APS-PGE2) or two amino groups (DAS-PGE3) were performed by dissolving the silane in tetrahydrofuran (THF) in a ratio 1.5 ml THF/g precursor silane, and heating at 50 °C during 24 h, allowing continuous evaporation of volatiles. The hydrolytic condensation was catalyzed by formic acid 85 wt.% (molar ratios:[HCOOH]/Si=3). Formic acid acts both as a catalyst and as water source, promoting the condensation through the formation of sililformates as intermediate species [23].

The characterization of the resulting amine-functionalized silsesquioxanes (ASSQO) has been reported in detail elsewhere [19-21]. Matrix-assisted ultraviolet laser desorption/ionization time-of-flight mass spectrometry (UV-MALDI-TOF MS) studies revealed that a mixture of silsesquioxane cages, $(RSiO_{1.5})_n$, which shows a narrow distribution of polyhedral structures is obtained. The main condensation products are structures containing 8-11 Si atoms in ASSQO1 and polyhedral structures containing 8 or 10 Si atoms in ASSQO2.

The ASSQO were incorporated into the BisTEG methacrylate resin at molar ratios [N/CQ] between 0 and 12 (Table 1). The optical clarity of the resins upon addition of the ASSQO indicates a good degree of dispersion of the nanofillers.

3.2. Photolysis of CQ in combination with amine-functionalized silsesquioxanes.

CQ acts in combination with hydrogen donors as tertiary amines, to generate radicals capable of initiating polymerization of methacrylate monomers. The mechanism of photodecomposition of CQ/amine systems has been reported in previous research [2,4], and is briefly described here. The CQ is excited under visible light irradiation, to the excited singlet state which converts to the reactive triplet state CQ* via inter-system crossing:

$$CQ + h\nu \rightarrow CQ^* \quad (1)$$

Free radicals are produced subsequently from two different reactions. CQ* can react with hydrogen donors such as tertiary amines (AH), to generate radicals by electron and proton transfer through a short lived charge-transfer intermediate complex (CTC) to give pinicol and amine derived radicals:

$$CQ^* + AH \rightarrow [CQ.....AH]^* \quad (CTC) \quad (2)$$

$$CTC \rightarrow CQH\bullet + A\bullet \quad (3)$$

Alternatively, photoreduction of CQ in the absence of coinitiator has been reported in monomers containing hydrogen donor groups such as methylene ether (–O–CH_2–) [4], and in these cases hydrogen abstraction can occur from the monomer (MH).

$$CQ^* + MH \rightarrow CQH\bullet + M\bullet \quad (4)$$

CQ displays an intense dark yellow colour due to the

presence of the conjugated diketone chromophore that absorbs at 470 nm. During irradiation of CQ and reduction of one of the carbonyl groups, the conjugation is destroyed, causing a blue shift of the remaining ketene's absorption and loss of the yellow colour. Thus, the photodecomposition of CQ in combination with different proportions of amine-functionalized silsesquioxanes was studied in BisTEG resin by monitoring the decrease in absorbance at the wavelength of the maximum absorption of CQ. Fig. 1 is a typical plot of spectral changes during irradiation of CQ/ASSQO1 in BisTEG resin showing a continuous decrease in absorbance with irradiation time. Irradiation of the sample for less than 60 s results in almost complete photobleaching of CQ.

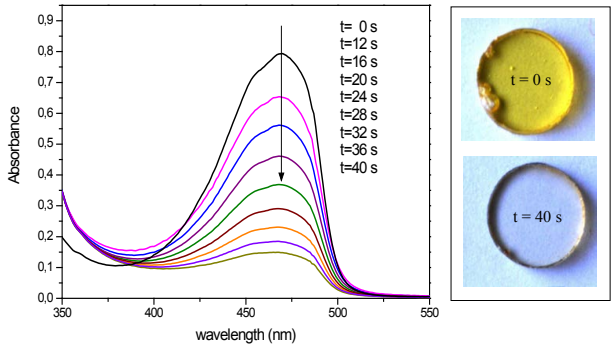

Fig.1. Typical spectral changes during irradiation of a resin containing 1 wt% CQ in combination with 15 wt% ASSQO1 and a sample before and after of photobleaching.

The rate of decomposition of CQ is related to the quantum yield and the radiation absorbed [24]:

$$-\frac{d\,CQ}{dt} = \frac{\Phi\, I_{abs}}{L} = \frac{\Phi\, I_0\,(1-e^{-\varepsilon LCQ})}{L} \qquad (5)$$

where CQ is the molar concentration of CQ, I_0 is the irradiance (in moles photons s^{-1} cm^{-2}) at the base of the sample, ε is the absorption coefficient of CQ equal to 2.302 times its extinction coefficient (42 ± 2 l/mol cm), L is the thickness of the sample, and Φ, which is usually termed the quantum yield of the photoinitiator consumption, is the fraction of photoinitiator reduced per absorbed photon. Integrating Eq. (5) yields:

$$ln\left[\frac{10^{\,\varepsilon LCQ}-1}{10^{\,\varepsilon LCQ_0}-1}\right] = -\Phi\,\varepsilon\, I_0\, t \qquad (6)$$

where ($\Phi\varepsilon I_0$) is the CQ rate constant for the photobleaching of CQ, and CQ_0 is the initial concentration of CQ. A satisfactory fit of experimental measurements of absorbance to a first-order kinetics for the decomposition of CQ in combination with ASSQO is observed (not shown). Table 1 shows the rate constant for the photobleaching of CQ, calculated from the slope of the lines (Eq. 6). It is seen that, for the range of ASSQO concentrations studied, the photobleaching rate of CQ was independent of the amine concentration. These results are in agreement with trends reported by Cook [2] for the photodecomposition of CQ/amine systems. The author found that if the intersystem crossing of the excited singlet to the triplet state is the rate determining step, then the consumption of CQ is independent of the amine concentration and only depends on the amine reactivity.

Table 1: Rate constants for the photobleaching of CQ in the presence of ASSQO. r is the molar ratio [N/CQ] and $k_i=\Phi\varepsilon I_0$ are the rate constants for the photobleaching of CQ for each ASSQO.

wt% ASSQO1	$k_1=\Phi\,\varepsilon\,I_0$ (s^{-1})	r=[N]/[CQ]	wt% ASSQO2	$k_2=\Phi\,\varepsilon\,I_0$ (s^{-1})
0	-	0	0	-
7.5	0.0778	3	5.5	0.0680
15	0.0781	6	11	0.0672
30	0.0782	12	22	0.0711

Statistically significant differences among the rate constants for the photobleaching of CQ in the presence of ASSQO1 or ASSQO2 are observed. This is an expected result, as the radical production in these reactions is markedly dependent on the structure of the electron donors, e.g. amines. Taking into account that the second amine group in the ASSQO2 is incorporated in the proximity of a polyhedral nanocage, it will have an important steric hindrance for the reaction with CQ (Scheme 1). Moreover, the amine groups in the ASSQO2 are more concentrated in specific places and consequently the statistics of reaction is low.

For a thick-section cure, it is advantageous to use photobleaching initiators in which light absorption by the initiator photoproducts is lower than that by the original photoinitiator molecule, thereby allowing more light to pass through the system [25-29]. Fig. 1 shows that the photolysis products of CQ/ASSQO are transparent at the irradiating wavelengths, consequently the consumption of the CQ leads to an increase in light intensity in the underlying lays. The clean and rapid photobleaching of CQ in combination with ASSQO makes this photoinitiator system very attractive for polymerization of thick sections.

3.3. Double bond conversion

The photoinitiation capability of CQ in combination with the ASSQO was assessed. Fig. 2 shows the progress of monomer conversion versus irradiation time in BisTEG resin with different amounts of ASSQO. The evolution of the polymerization reaction photoinitiated by the pair CQ/ethyl-4-dimethylami-

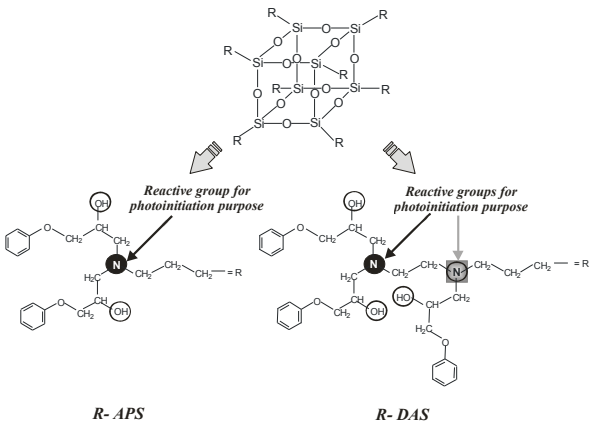

Scheme 1: Structure of the R-substituent in (a) the APS-derived silsesquioxanes, (b) the DAS-derived silsesquioxanes.

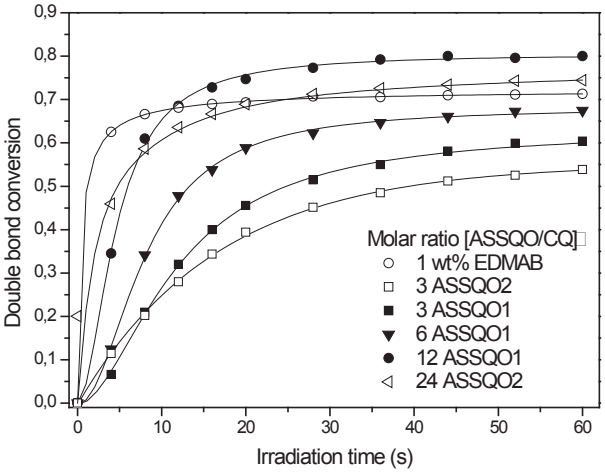

Fig.2: Monomer conversion (measured from NIR spectra) versus irradiation time for a 2 mm thick BisTEG resin specimen containing 1 wt% CQ in combination with different molar ratios of ASSQO1 and ASSQO2. The conversion in a photoactivated resin with CQ/EDMAB is shown for comparison (circles).

nobenzoate (EDMAB), which showed an optimum polymerization rate [3], is shown for comparison in the same plot. For related ketone/amine photoinitiation systems [3–6] it is generally considered that the amine radical is responsible for initiating the polymerization and that the radical formed from the ketone is not an efficient initiator due to a steric hindrance effect. Thus, the number and type of active amine radical determine the photopolymerization rate. Plots in Fig. 2 show that amine groups present in both ASSQO are efficient co-initiators for CQ because a fast reaction and high conversions are obtained after 60 s irradiation at 600 mW/cm^2. As expected, the polymerization rate increases with the ASSQO content as the number of amine radicals increases. The influence of the mass fraction of ASSQO on the final monomer conversion is attributed to the temperature rise in the sample due to the exothermic reaction. A higher sample temperature increases the mobility of the reaction environment (i.e. monomer, radical and polymer) and consequently increases the reaction rate parameters. In addition, once the photocuring temperature approaches the glass transition temperature the material vitrifies and the reaction is virtually stopped, limiting in this way the maximum conversion reached. Therefore, the samples containing higher proportions of ASSQO attained a higher temperature and consequently a higher limiting conversion. This result is observed for both ASSQO studied (Fig. 2).

In Fig. 2 it is seen that the polymerization rate by using CQ in combination with ASSQO was slower than that corresponding to the CQ/EDMAB pair. To reach the same final conversion as that reached in the resin containing 1 wt% CQ in combination with equimolar proportion of EDMAB, the molar ratio N:CQ must by higher than 6. The different photoinitiation efficiencies of formulations containing CQ/EDMAB or CQ/ASSQO may be attributed to structural effects on the recombination rate of radicals and on the radical reactivity toward the monomer double bond [3]. In this regard, EDMAB has two methyl groups attached to nitrogen atom, whereas SSQO has methylene groups shielded by the rest of the substituent. Conformational mobility of the amine radicals of ASSQO, which increases the steric hindrance for the radical addition might explain the observed differences [30]. In addition, the mobility of EDMAB is expected to be higher than that of SSQO structures due to the comparatively lower molecular weight of the former. Another factor to be considered when comparing the reactivity of systems photoactivated with CQ/EDMAB or CQ/ASSQO (Fig.2) is the dilution effect after addition of SSQO; which act as an unreactive diluent. The polymerization rate of the resin containing higher molar ratio [N/CQ] was slower than that of CQ/EDMAB at early stage. However, at some seconds irradiation the reversed trend was observed and the conversion of BisTEG photoactivated with CQ/ASSQO was slightly greater than that of BisTEG containing CQ/EDMAB. Again, the trend observed at early stage is explained by a comparatively lower mobility of the macromolecular ASSQO in the reaction medium. Moreover, at higher conversion, the intramolecular H-abstraction between amino groups and CQ in ASSQO is less affected by vitrification of the resin than that in the CQ/EDMAB because of the higher local amino concentration in ASSQO, which makes CQ/ASSQO photoinitiator systems yield more active species. Moreover, from Fig. 2 it is seen that there is an increase in the conversion when ASSQO1

was used.

3.4 Mechanical properties

The applied load versus strain curves in flexural tests exhibited a linear relationship over the whole range of strain and all specimens fractured catastrophically in the linear regime. Tables 2 and 3 show the flexural modulus (E) and the flexural strength (σ_f) of materials prepared from BisTEG resin containing different proportions of ASSQO1 and ASSQO2 respectively. As it was shown in Fig. 2, the polymerization of dimethacrylates in the absence of external heating leads to glassy resins in which only some of the available double bonds are reacted. Before the completion of conversion, the vitrification phenomenon decelerates the reaction to a hardly perceptible rate [31]. The presence of non-reacted monomer can have a plasticizing effect on the polymer, thereby altering the overall properties of the hardened material. Thus, the mechanical behaviour of methacrylate polymers containing ASSQO is influenced in a complex way by the presence of the ASSQO and the residual monomer. The flexural test results show that the presence of ASSQO1 resulted in a significant decrease in the flexural modulus. By the addition of 30 wt% ASSQO1, the flexural modulus decreased by approximately 25 % and 37 % in samples with and without post-curing treatment respectively, compared with the unmodified resin. A no significant change in the flexural modulus has been seen in the presence of ASSQO2. Conversely, the addition of ASSQO1 and ASSQO2 produced no apparent change in the flexural strength. The post-curing treatment at 120 °C increases the monomer conversion and reduces the plasticizing effect of the non-reacted monomer on the mechanical behaviour of the nanocomposites. Thus, the higher values of flexural modulus and flexural strength of samples subjected to a post-curing treatment are attributed to a reduced amount of non-reacted monomer. The high data scatter observed in flexural strength values is associated to a brittle rupture of the test specimens [32-33]. Brittle fracture occurs due to the propagation of a crack in the material. Flaws of variable sizes, shapes and orientations with respect to the applied load are possible. Hence, variable crack sizes and their orientations with respect to the applied load can account for the observed scatter of fracture strengths, when nominally identical specimens are tested under nominally identical loading conditions [32-33].

The most striking behaviour displayed by BisTEG resins modified with ASSQO is seen in the stress-strain curves from compression tests. Tables 2 and 3 show the compressive yield strength (σ_y) in compression tests of the BisTEG resin containing different proportions of ASSQO1 and ASSQO2 respectively, as well as the unmodified BisTEG resin for comparison. It is observed a significant decrease in the compressive strength (σ_y) of BisTEG with increasing content of ASSQO1 and no differences with the content of ASSQO2. As shown in Fig 2 the conversion of methacrylate monomers increases with the content of ASSQO. Consequently, the marked reduction in the yield stress with increasing ASSQO1 content can not be associated to the plasticization caused by the unreacted monomer.

Different from traditional micro-reinforced composites, in nanostructured materials the surface effect becomes significant and might have a substantial influence on the overall properties. It is conceivable that debonding of ASSQO cages from the polymer gives rise to nanovoids. These nanovoids would allow the methacrylate matrix to yield and deform plastically thereby reducing the yield stress values [34]. The different trends in the mechanical properties of resins

Table 2: Flexural modulus (E), flexural strength (σ_f) and compressive yield strength (σy) of BisTEG monomer modified with different proportions of ASSQO1.

wt% ASSQO2	E (GPa)	σ_f (MPa)	σ_y (MPa)	E_{post} (GPa)	$\sigma_{f\ post}$ (MPa)	$\sigma_{y\ post}$ (MPa)
0	2.8 (±0.20)	81.7 (±12.7)	110.8 (±1.9)	3.6 (±0.16)	113.8 (±10.2)	124.7 (±6.4)
5.5	1.9 (±0.32)	89.2 (±18)	102.3 (±2.7)	2.9 (±0.33)	100.5 (±31.3)	117.5 (±2.7)
11	2.2 (±0.29)	117.9 (±14.1)	101.4 (±3.4)	3.6 (±0.12)	119.8 (±22.1)	124.4 (±1.1)
22	2.1 (±0.13)	110.4 (±19.8)	102.1 (±2.9)	3.6 (±0.10)	121.7 (±30.6)	112.2 (±1.8)

Table 3: Flexural modulus (E), flexural strength (σ_f) and compressive yield strength (σy) of BisTEG monomer modified with different proportions of ASSQO2.

wt% ASSQO2	E (GPa)	σ_f (MPa)	σ_y (MPa)	E_{post} (GPa)	$\sigma_{f\ post}$ (MPa)	$\sigma_{y\ post}$ (MPa)
0	2.8 (±0.20)	81.7 (±12.7)	110.8 (±1.9)	3.6 (±0.16)	113.8 (±10.2)	124.7 (±6.4)
5.5	1.9 (±0.32)	89.2 (±18)	102.3 (±2.7)	2.9 (±0.33)	100.5 (±31.3)	117.5 (±2.7)
11	2.2 (±0.29)	117.9 (±14.1)	101.4 (±3.4)	3.6 (±0.12)	119.8 (±22.1)	124.4 (±1.1)
22	2.1 (±0.13)	110.4 (±19.8)	102.1 (±2.9)	3.6 (±0.10)	121.7 (±30.6)	112.2 (±1.8)

photoactivted with DAS-derived silsesquioxanes and APS-derived silsesquioxane may be attributed to the following factors. First, the R-substituent in the DAS-derived silsesquioxanes contains two amino groups while the R group in the APS-derived silsesquioxanes contains one amino group (Scheme 1). Second, the molar mass of the R-substituent in the DAS-derived silsesquioxanes (551 g) is about 1.5 times greater than that of the APS-derived silsesquioxane (358 g). Consequently, in order to reach similar photoinitiation capability in resins photoinitiated with DAS-derived silsesquioxanes and APS-derived silsesquioxanes, the number of polyhedral nanocages required in the former is lower than that required in the latter. Thus, the comparatively higher strength of resins containing DAS-derived silsesquioxanes is attributed to the presence of lower amount of potential deformation sites. Fig. 2 shows that the final monomer conversion increases with the content of ASSQO. Therefore, the higher number of nanovoids in resins containing higher proportion of ASSQO is compensated by a lower residual monomer content; which acts as a plasticizer. Because of these opposite effects, the flexural and compressive properties are unchanged with increasing amounts of ASSQO.

4. Conclusions

Polyhedral oligomeric silsesquioxanes functionalized with one or two side-chains amino groups (ASSQO) were prepared by hydrolytic condensation of both APS-PGE2 and DAS-PGE3 catalyzed by formic acid.

ASSQO were incorporated into BisTEG methacrylate resins at molar ratio [amine/CQ] between 0 and 12 for visible light polymerization. The optical clarity of the resins upon addition of the ASSQO indicates a good degree of dispersion of the nanofillers.

From results obtained in this study it emerges that radicals produced by the photodecomposition of ASSQO induce polymerization and this process is comparable to that of CQ/amine commercial. The high photobleaching rate and the high polymerization rates make the CQ/ASSQO photoinitiator system attractive as photoinitiator of methacrylate monomers.

Moreover, depending on the chemical structure of the pendant of ASSQO that act as coinitiator of CQ, the flexural or the compressive properties of the final material could or non be compromised.

Acknowledgements

The financial support provided by the CONICET and the ANPCyT is gratefully acknowledged. The authors are grateful to Esstech for the generous donation of the Bis-GMA monomer used in this study.

References:

1. **Valderas, C.; Bertolotti, C; Previtali, M; Encinas M..** Influence of the amine structure on the polymerization of methyl methacrylate photoinitiated by aromatic ketone/amine. *J. Polym. Sci. A Polym. Chem.,* **40** (2002), 2888-2893.
2. **Cook WD.** Photopolymerization kinetics of dimethacrylates using the camphorquinone amine initiator system. *Polymer,* **33** (1992), 600-609.
3. **Schroeder WF, Vallo CI.** Effect of different photoinitiator systems on conversion profiles of a model unfilled light-cured resin. *Dent Mater,* **23** (2007), 1313–21.
4. **Jakubiak J, Allonas X, Fouassier JP, Sionkowska A, Andrzejewska E, Linden LA, et al.** Camphorquinone-amines photoinitating systems for the initiation of free radical polymerization. *Polymer,* **44** (2003), 5219–26.
5. **Schroeder WF, Arenas G, Vallo CI.** Monomer conversion in a light-cured dental resin containing 1-phenyl-1,2-propanedione photosensitizer. *Polym Int,* **36** (2007)1099-1105.
6. **Schroeder W, Cook WD, Vallo CI.** Photopolymerization of N,N dimethyl aminobenzyl alcohol as amine co-initiator for light-cured dental resins. *Den Mater,* **24** (2008), 686–93.
7. **Wang K, Yang D, Xiao M, Chen X, Lu F, Nie J.** Sesamin as a co-initiator for unfilled dental restorations *Acta Biomaterialia,* **5** (2009), 2508–17.
8. **Wua G, Nie J.** Synthesis and evaluation of ethylene glycol 3-diethylamino-propionate methacrylate as a polymerizable amine coinitiator for dental application. *Dent Mater,* **23** (2007), 623–629.
9. **Sanchez C, Ribot F, Lebeau B,** Molecular design of hybrid organic-inorganic nanocomposites synthesized via sol-gel chemistry *J. Mater. Chem.,* **9** (1999), 35-44.
10. **Zhang W, Zhuang X, Li X, Lin Y, Bai J, Chen Y.** Preparation and characterization of organic/inorganic hybrid polymers containing polyhedral oligomeric silsesquioxane via RAFT polymerization. *React Funct Polym,* **69** (2009), 124-129.
11. **Kawakami Y.** Structural control and functionalization of oligomeric silsesquioxanes. *React Funct Polym,* **67** (2007), 1137-1147.
12. **Ikeda M, Saito H.** Improvement of polymer performance by cubic-oligosilsesquioxane. *React Funct Polym.,* **27** (2007), 1148-1156.
13. **Asmussen SV, Vallo CI.** Characterization of light-cured dimethacrylate resins modified with silsesquioxanes. *J Mater Sci.,* **46** (2011), 2308-2317.
14. **Asmussen SV, Vallo CI.** Synthesis of silsesquioxanes based in (3-methacryl oxypropyl)-trimethox-

ysilane using methacrylate monomers as reactive solvents. *Eur Polym J.,* **46** (2010), 1815-1823.

15. **Briche S, Riassetto D, Gastaldin C, Lamarle C, Dellea O, et al.** Sol-gel processing and UVA patterning of epoxy-based hybrid organic-inorganic thin films. *J Mater Sci,* **43** (2008), 5809-5822.
16. **Soh MS, Yap AUJ, Sellinger A.** Methacrylate and epoxy functionalized nanocomposites based on silsesquioxane cores for use in dental applications. *Eur Polym J,* **43** (2007), 315-327.
17. **Oubaha M, Copperwhite R, Boothman C, Ovsianikov A, Kiyan R et al.** Influence of hybrid organic-inorganic sol-gel matrices on the photophysics of amino-functionalized UV-sensitizers - *J Mater Sci,* **46** (2011), 400-408.
18. **dell'Erba IE, Williams RJJ.** Synthesis of oligomeric silsesquioxanes functionalized with (β-carboxyl) ester groups and their use as modifiers of epoxy networks. *Eur Polym J.,* **43** (2007), 2759-2767.
19. **dell' Erba IE, Fasce DP, Williams RJJ, Erra-Balsells R, Fukuyama Y, Nonami H.** Poly(silsesquioxanes) derived from the hydrolytic condensation of organotrialkoxy silanes containing hydroxyl groups. *J Organomet Chem,* **686** (1-2) (2002), 42-51.
20. **D.P. Fasce, R.J.J. Williams, F. Mechin, J.P. Pascault, M.F. Llauro, R. Petiaud,** Synthesis and characterization of polyhedral silsesquioxanes bearing bulky functionalized substituents, *Macromolecules* **32** (1999) 4757-4763.
21. **D.P. Fasce, R.J.J. Williams, R. Erra-Balsells, Y. Ishikawa, H. Nonami,** One-step synthesis of polyhedral silsesquioxanes bearing bulky substituents: UV-MALDI-TOF and ESI-TOF mass spectrometry characterization of reaction products. *Macromolecules* **34** (2001) 3534-3539.
22. **Baney RH, Itoh M, Sakakibara A, Suzuki T.** Silsesquioxanes, *Chem. Rev.,* **95** (1995), 1409.
23. **Sharp K.** A two-component, non-aqueous route to silica gel-code:A7. *J Sol–Gel Sci Technol,* **2** (1994), 35–41.
24. **Odian G.** Principles of polymerization. 3rd edition NY: Wiley, (1991), 222–229.
25. **Miller G, Gou I, Narayanan V, .Scranton AJ,** Modeling of Photobleaching for the Photoinitiation of Thick Polymerization Systems. *J Polym Sci Part A: Polym Chem,* **40** (2002), 793-808.
26. **Kenning NS, Dane Kriks, Mohammed El-Maazawi and Alec Scranton.** Spatial and temporal evolution of the photoinitiation rate for thick polymer systems illuminated with polychromatic light. *Polym Int,* **57** (2006), 994-1006.
27. **Kenning NS, Ficel BA, Hoppe CC, Scranton A,** Spatial and temporal evolution of the photoinitiation rate for thick polymer systems illuminated by polychromatic light: selection of efficient photoinitiators for LED or mercury lamps. *Polym Int,* **57** (2008), 1134-1140.
28. **Asmussen SV, Arenas G, Cook WD, Vallo CI.** Photoinitiation rate profiles during polymerization of a dimethacrylate-based resin photoinitiated with Camphorquinone/ amine. Influence of initiator photobleaching rate. *Eur Polym J.,* **45** (2009), 515-522.
29. **Asmussen SV, Arenas G, Cook WD, Vallo CI.** Photobleaching of Camphorquinone during polymerization of dimethacrylate-based resins. *Dent Mater,* **25** (2009), 1603-1611.
30. **Brulé C., Hoffmann N.,** Stereosolectivity intermolecular addition of ketyl radicals generated from ketones by photoinduced electron transfer. *Tetrahedron Lett.,* **43** (2002), 69-72.
31. **Vallo CI.** Residual Monomer Content in bone Bements Based on PMMA. *Polym Int,* **49** (2000), 831-838.
32. **Vallo CI.** Influence of Load Type on Flexural Strength of a Bone Cement Based on PMMA. *PolymTest,* **21** (2002), 793-800.
33. **Giannotti MI, Galante MJ, Oyanguren PA, Vallo CI.** Role of the intrinsic flaws upon the flexural strength of a thermoplastic modified epoxy resin. *Polym Test,* **22** (2003), 429-437.
34. **Asmussen S., dell' Erba I., Schroeder W., Vallo C.** Photopolymerization of methacrylate monomer using polyhedral silsesquioxanes bearing side-chain amines as photoinitiator. *Eur Polym J.,* **48** (2012), 309-317.